DOI: 10.1021/ma901757w

Macromolecules
ARTICLE

Directly Probing Molecular Ordering at the Buried Polymer/Metal Interface

Xiaolin Lu,[†,‡] Dawei Li,[†,‡] Cornelius B. Kristalyn,[‡] Jianglong Han,[†] Nick Shephard,[§] Susan Rhodes,[§] Gi Xue,*[,†] and Zhan Chen*[,‡]

[†]*Department of Polymer Science, Nanjing University, Nanjing, People's Republic of China 210093,* [‡]*Department of Chemistry, University of Michigan, 930 North University Avenue, Ann Arbor, Michigan 48109, and* [§]*Specialty Chemicals Business, Materials Science Technology Platform, Dow Corning Corporation, 2200 W. Salzburg Road, Midland, Michigan 48686*

Received August 5, 2009; Revised Manuscript Received September 21, 2009

ABSTRACT: We developed a methodology to directly probe molecular ordering at the buried polymer/metal interface. Using sum frequency generation (SFG) vibrational spectroscopy, we observed ordering of ester methyl groups at the buried poly(methyl acrylate) (PMA)/silver (Ag) interface. In order to directly probe the PMA/Ag interface, we collected SFG signal from a thin PMA film sandwiched between a fused silica substrate and a silver surface. It was found that the observed SFG signal intensity does not depend on the PMA film thickness. According to the calculated Fresnel coefficients of the fused silica/PMA and PMA/Ag interfaces with PMA films of different thicknesses, it was shown that SFG signals are solely contributed by the PMA/Ag interface. Further studies indicated that the ester methyl groups at the PMA/Ag interface tilt away from the Ag surface.

1. Introduction

Understanding the molecular structure at the buried interface between two bulk phases is of great importance because the molecular structure can be correlated to the macroscopic interfacial properties like adhesion, friction, wettability, and biocompatibility.[1−4] No matter whether the interaction at the interface between the two bulk phases is attractive or repulsive, the molecular ordering at the interface is usually different from those in the bulk phases. For example, for a polymer/metal interface, especially an amorphous polymer/metal interface, because of the soft and "random" nature of the polymer and the rigid nature of the metal, we should expect a higher interfacial order of the polymer at the polymer/metal interface compared to that in the polymer bulk. To detect this "ordering" at a buried interface, a nondestructive and mono- or submonolayer interface sensitive technique is needed. Here we will demonstrate that using sum frequency generation (SFG) vibrational spectroscopy, we can "directly" probe such an interfacial order at the polymer/metal interface *in situ*. Understanding structures at the polymer/metal interfaces is essential for many important applications such as anticorrosion polymer coatings and polymer adhesives in modern microelectronics.

SFG has been extensively applied to study molecular structures of surfaces and interfaces, including polymer surfaces.[5−41] In order to use SFG to investigate a buried interface, it is required that at least one of the two contacting bulk materials is transparent to both visible and infrared beams so that the SFG input beams can reach the buried interface. SFG has been successfully applied to examine buried solid/solid interfaces.[16,19,27,30,31,33,37,39−41] However, polymer/metal interfaces have rarely been investigated using SFG. The uniqueness of this research is that we showed SFG can probe polymer/metal interfaces directly. It is not necessary to collect SFG spectra from polymer films (on metal) with different thicknesses, as we did previously.[42] Previously, we have successfully applied SFG to examine buried polymer/metal interfaces, using the poly(methyl methacrylate) (PMMA)/silver (Ag) interface as a model.[42] In that study, SFG spectra were collected from a PMMA film deposited on a silver surface. To ensure that the input beams can reach the PMMA/Ag interface, PMMA thin films had to be used. SFG signals collected from such a sample were contributed by the PMMA/air interface, the PMMA/Ag interface, and the nonresonant background. In order to deconvolute the SFG signals of the PMMA/Ag interface from the observed "overall" SFG signals, SFG signals were collected from PMMA films with varied thicknesses. With PMMA films of different thicknesses, SFG signals contributed from the two interfaces can interfere with each other in different ways. Then the observed "overall" SFG spectra can be fitted using such thickness-dependent interferences; from these fitting results the contribution from the PMMA/Ag interface can be deduced.[42] This method is quite time-consuming because SFG studies on PMMA with a variety of thicknesses have to be performed. Also, achieving satisfactory spectral fitting for several SFG spectra (of films with different thicknesses) simultaneously with the same set of fitting parameters (only the film thickness can be varied) is sometimes quite challenging.

In this paper, we developed a new methodology to apply SFG to directly probe the buried polymer/metal interface using a poly(methyl acrylate) (PMA)/Ag interface as a model. Instead of depositing a thin polymer film on a silver surface, here we sandwiched a thin polymer film between a fused silica surface and a silver surface. We found that SFG signal contributed from the polymer/fused silica interface is negligible. Therefore, SFG signal collected from the polymer film is solely contributed from the polymer/metal interface. Thus, it is not necessary to make polymer films with varied thicknesses to probe the polymer/metal interface, as done in the previous study. Instead, we can directly probe the polymer/metal interface using SFG. Indeed, here we

*To whom all correspondence should be addressed: e-mail xuegi@nju.edu.cn (G.X.); e-mail zhanc@umich.edu, Fax 734-647-4865 (Z.C.).

 Published on Web 10/14/2009

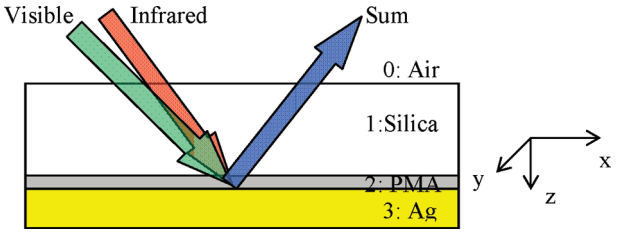

Figure 1. Schematic showing the SFG experimental geometry for a sandwiched PMA thin film between a fused silica window substrate and a silver substrate.

showed that SFG signals collected from the PMA films with varied thicknesses are more or less similar; they do not depend on the film thickness. This also indicates that here SFG signals from the possible bulk contribution beyond the electric-dipole approximation are negligible; otherwise, thickness-dependent SFG signals should be observed.

2. Experimental Section

PMA ($M_w \approx 40\,000$) was purchased from Scientific Polymer Products, Inc. Fused silica windows of 1 in. diameter and $^1/_8$ in. thickness were ordered from Esco Products, Inc. Fused silica substrates were treated sequentially by a sulfuric acid bath saturated with potassium dichromate, air plasma, and a piranha solution bath (a mixed solution with 3:7 volume ratio of 30 wt % H_2O_2 solution and 98 wt % H_2SO_4). PMA films with different thicknesses were prepared by spin-coating the PMA toluene solution onto the cleaned fused silica substrates. Film thickness was controlled by adjusting the spin speed and the polymer solution concentration. After the PMA samples were annealed at 80 °C for 1 h (the glass transition temperature, T_g, of PMA is 5 °C), we deposited a 500 nm layer of silver (Ag) on top of the polymer film using an electron-beam evaporator (1 nm/s, Cooke Evaporator, Cooke Vacuum Products). The PMA film sandwiched between the fused silica surface and the deposited Ag film was annealed at 80 °C again for 1 h.

SFG theories as well as the SFG setup used in our laboratory have been reported extensively in previous publications[5−42] and will not be repeated here. To collect SFG signals, we adopted a "face-down" experimental geometry in our SFG experiments in this study (Figure 1). In this geometry, the SFG input visible and infrared (IR) beams come from the silica window side. They go through the silica window substrate and then overlap spatially and temporally at the PMA/Ag interface. The visible and IR input angles (before reaching the silica window) are 60° and 54°, respectively, with beam diameters of ~500 μm. The pulse energies of the visible and IR beams were adjusted to 5 and 90 μJ, respectively, to avoid burning the samples. In this study, SFG spectra were collected using ssp (s-polarized SFG signal, s-polarized input visible, and p-polarized input infrared beam) and ppp polarization combinations.

3. Results and Discussion

Previously, we have collected SFG spectra from the PMA surface in air as a comparison when we investigated surface structures of PMMA in air.[13] In air for both PMA and PMMA, ester methyl groups dominate the surfaces. These surface dominating ester methyl groups tilt toward the surface normal. As we mentioned above, we have studied the PMMA/Ag interface by collecting SFG spectra of PMMA films with varied film thicknesses on Ag. SFG signals from the buried PMMA/Ag interface can be deconvoluted from the observed overall SFG signals (which were contributed from both the PMMA/air interface and the PMMA/Ag interface). Usually the SFG signals contributed from the polymer/air interface are strong. Therefore, the deconvolution needs to be done very carefully; otherwise,

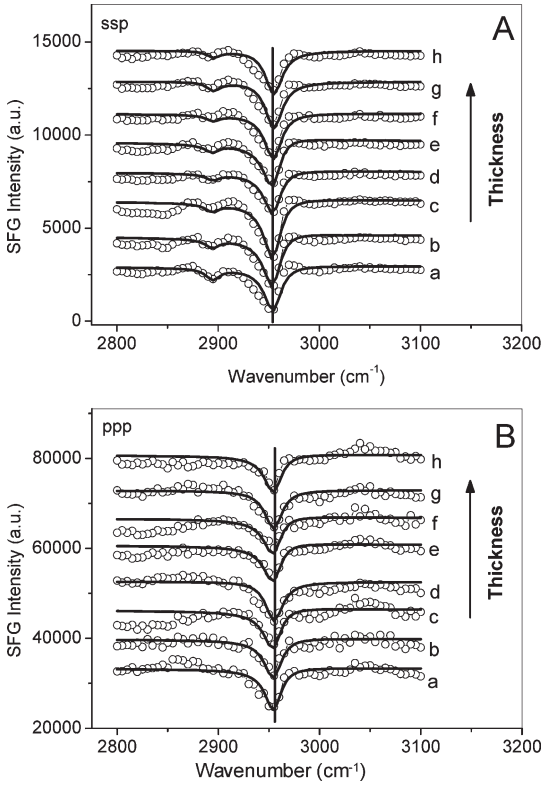

Figure 2. SFG spectra of the PMA thin films sandwiched between the silica window substrate and Ag surface; the PMA thin film thicknesses of sample a, b, c, d, e, f, g, and h are 19, 25, 41, 67, 89, 111, 136, and 153 nm, respectively; the spectra have been offset for clarity. (A) ssp spectra; (B) ppp spectra.

substantial errors may be induced in the data analysis. It was found that the PMMA/Ag interface is also dominated by the ester methyl groups. They tilt away from the Ag surface with a smaller orientation angle versus the surface normal (lie down more) compared to those at the PMMA/air interface.

Here SFG spectra were collected from a PMA thin film sandwiched between a fused silica surface and a silver surface. For such a sample, both the PMA molecules at the silica/PMA and PMA/Ag interfaces may generate resonant SFG signals because of the broken inversion symmetry at the two interfaces. Assuming that these two interfaces are azimuthally isotropic,[43] the SFG ssp signal is then contributed by the second-order nonlinear susceptibility tensor component χ_{yyz} of the vibrational modes at the two interfaces, as shown in eq 1:

$$\chi^{(2)}_{\mathrm{eff,ssp}} = F^{\mathrm{silica/PMA}}_{yyz}\chi^{\mathrm{silica/PMA}}_{yyz} + F^{\mathrm{PMA/Ag}}_{yyz}\chi^{\mathrm{PMA/Ag}}_{yyz} + \chi^{\mathrm{NR}}_{\mathrm{ssp}} \quad (1)$$

$\chi^{(2)}_{\mathrm{eff,ssp}}$ is the effective second-order nonlinear susceptibility tensor component probed using the ssp polarization combination of the input and output beams; $\chi^{\mathrm{silica/PMA}}_{yyz}$ and $\chi^{\mathrm{PMA/Ag}}_{yyz}$ are the second-order nonlinear susceptibility tensor components of the vibrational modes of PMA functional groups at the silica/PMA and PMA/Ag interfaces, respectively; $F^{\mathrm{silica/PMA}}_{yyz}$ and $F^{\mathrm{PMA/Ag}}_{yyz}$ are the apparent Fresnel coefficients for the silica/PMA and PMA/Ag interfaces, respectively; $\chi^{\mathrm{NR}}_{\mathrm{ssp}}$ is the nonresonant background mainly arising from the Ag substrate.

Figure 2 shows the ssp (A) and ppp (B) spectra of the sandwiched PMA films with different thicknesses, and Table 1 shows the fit parameters for such spectra. The ssp spectra collected from the PMA samples with different film thicknesses

Table 1. Fit Parameters for SFG Spectra Collected from the PMA Thin Films Sandwiched between a Silica Window Substrate and a Silver Surface (Figure 2): (A) for ssp; (B) for ppp

A

	2955 cm^{-1}		2895 cm^{-1}			
thickness (nm)	A_i	Γ_i	A_i	Γ_i	χ_{NR}	phase (rad)
19	305 ± 12	10	48 ± 5	8	54 ± 2	−1.4 ± 0.1
25	332 ± 15	10	33 ± 4	8	57 ± 3	−1.3 ± 0.2
41	342 ± 13	10	28 ± 4	8	59 ± 4	−1.4 ± 0.1
67	300 ± 11	10	25 ± 3	8	52 ± 3	−1.4 ± 0.1
89	296 ± 17	10	30 ± 4	8	56 ± 3	−1.3 ± 0.1
111	293 ± 13	10	23 ± 3	8	55 ± 3	−1.4 ± 0.1
136	286 ± 15	10	33 ± 3	8	58 ± 2	−1.5 ± 0.2
153	290 ± 14	10	25 ± 4	8	55 ± 2	−1.5 ± 0.1

B

	2955 cm^{-1}			
thickness (nm)	A_i	Γ_i	χ_{NR}	phase (rad)
19	268 ± 21	10	182 ± 3	−1.4 ± 0.1
25	259 ± 17	10	181 ± 4	−1.4 ± 0.1
41	241 ± 26	10	193 ± 5	−1.3 ± 0.2
67	279 ± 23	10	170 ± 4	−1.6 ± 0.1
89	249 ± 17	10	179 ± 6	−1.3 ± 0.1
111	245 ± 24	10	178 ± 2	−1.3 ± 0.1
136	250 ± 17	10	184 ± 3	−1.6 ± 0.1
153	251 ± 20	10	178 ± 5	−1.4 ± 0.1

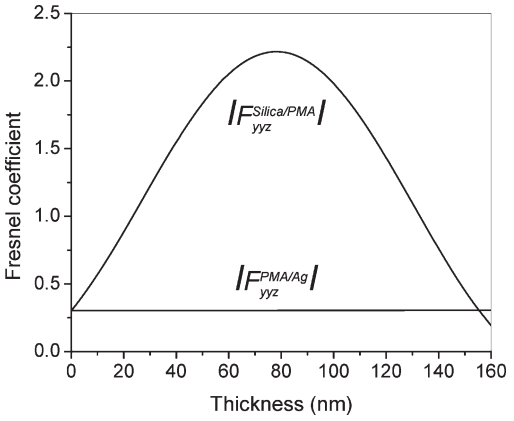

Figure 3. Absolute Fresnel coefficients calculated for the silica/PMA interface and the PMA/Ag interface as a function of the PMA thickness for the ssp spectra.

are dominated by a negative peak at 2955 cm^{-1}. This peak is assigned to the ester methyl symmetric stretching (ss) mode. For SFG ppp spectra collected from the PMA films with different film thicknesses, only a discernible negative peak at 2955 cm^{-1} is observed. The observed SFG spectra do not depend on the film thickness. This is different from the signals collected from the polymer films deposited on a Ag surface with different thicknesses which we studied previously.[42]

We calculated both $|F^{silica/PMA}_{yyz}|$ and $|F^{PMA/Ag}_{yyz}|$ as a function of the film thickness using a thin-film model[42,44,45] (Figure 3). It was found that $|F^{PMA/Ag}_{yyz}|$ remains more or less the same (~0.31) when the film thickness is varied, while $|F^{silica/PMA}_{yyz}|$ shows substantial film thickness dependence. The constant $|F^{PMA/Ag}_{yyz}|$ can be interpreted by the similar refractive indices of fused silica and PMA. Because of the similar refractive indices, the SFG signal generated from the PMA/Ag interface would not have multiple reflections inside the PMA film, leading to no thickness dependence. We believe that the observed SFG ssp spectra should be contributed from the PMA/Ag interface because they are not dependent on the film thickness, matching with the calculated Fresnel coefficient at the PMA/Ag interface. If they are generated by the silica/PMA interface or both the silica/PMA and PMA/Ag interfaces, SFG spectra should be dependent on the film thickness.

Table 1 shows that χ^{NR}_{ssp} does not depend on the PMA film thickness as well. We believe that χ^{NR}_{ssp} is mainly contributed from the Ag substrate surface. We also noticed that the phase difference between χ^{NR}_{ssp} and the negative peak at 2955 cm^{-1} is constant, independent of the film thickness. This also suggests that the 2955 cm^{-1} peak in the ssp SFG spectra (Figure 2A) are dominated by the PMA/Ag interface. Otherwise, a substantial phase change of this peak relative to that of the nonresonant background should be observed.

The SFG ppp polarization combination of the input and output laser beams detects the second-order nonlinear susceptibility tensor components of χ_{xxz}, χ_{xzx}, χ_{zxx}, and χ_{zzz}, at the two interfaces (silica/PMA and PMA/Ag), as shown in eq 2:

$$\chi^{(2)}_{eff,ppp} = F^{silica/PMA}_{xxz}\chi^{silica/PMA}_{xxz} + F^{PMA/Ag}_{xxz}\chi^{PMA/Ag}_{xxz} + F^{silica/PMA}_{xzx}\chi^{silica/PMA}_{xzx} + F^{PMA/Ag}_{xzx}\chi^{PMA/Ag}_{xzx} + F^{silica/PMA}_{zxx}\chi^{silica/PMA}_{zxx} + F^{PMA/Ag}_{zxx}\chi^{PMA/Ag}_{zxx} + F^{silica/PMA}_{zzz}\chi^{silica/PMA}_{zzz} + F^{PMA/Ag}_{zzz}\chi^{PMA/Ag}_{zzz} + \chi^{NR}_{ppp} \quad (2)$$

where $\chi^{(2)}_{eff,ppp}$ is the effective second-order nonlinear susceptibility tensor component detected using the ppp polarization combination; $\chi^{silica/PMA}_{xxz}$, $\chi^{silica/PMA}_{xzx}$, $\chi^{silica/PMA}_{zxx}$, $\chi^{silica/PMA}_{zzz}$, $\chi^{PMA/Ag}_{xxz}$, $\chi^{PMA/Ag}_{xzx}$, $\chi^{PMA/Ag}_{zxx}$, and $\chi^{PMA/Ag}_{zzz}$ are the corresponding tensor components of the vibrational modes of PMA molecules at the silica/PMA and PMA/Ag interfaces, respectively; $F^{silica/PMA}_{xxz}$, $F^{PMA/Ag}_{xxz}$, $F^{silica/PMA}_{xzx}$, $F^{PMA/Ag}_{xzx}$, $F^{silica/PMA}_{zxx}$, $F^{PMA/Ag}_{zxx}$, $F^{silica/PMA}_{zzz}$, and $F^{PMA/Ag}_{zzz}$ are the apparent Fresnel coefficients of the fused silica/PMA and PMA/Ag interfaces, respectively; χ^{NR}_{ppp} is the nonresonant background.

We also proved that the ester methyl symmetric stretching peak at 2955 cm^{-1} in the ppp spectra is dominantly contributed by the PMA molecules at the PMA/Ag interface. In the case of an azimuthally isotropic interface, only four independent nonvanishing components for the second-order nonlinear susceptibility[43] exist:

$$\chi_{xxz} = \chi_{yyz}, \quad \chi_{xzx} = \chi_{yzy}, \quad \chi_{zxx} = \chi_{zyy}, \chi_{zzz} \tag{3}$$

From our above discussion on the ssp spectra, we can deduce that $\chi_{yyz}^{PMA/Ag} \gg \chi_{yyz}^{silica/PMA}$ (because signals can only be detected from the PMA/Ag interface in ssp spectra); we thus have $\chi_{xxz}^{PMA/Ag} \gg \chi_{xxz}^{silica/PMA}$. The ester methyl group can be treated as having a C_{3v} symmetry.[46,47] According to the relationship between the measured χ components in the lab-fixed coordinate system and the molecule-fixed coordinate system for the symmetric stretching mode in C_{3v} symmetry,[47] we have

$$\chi_{xxz} = \chi_{yyz} = \frac{1}{2} N_s \alpha_{ccc} [\cos\theta(1 + r) - \cos^3\theta(1 - r)] \tag{4}$$

$$\chi_{xzx} = \chi_{zxx} = \chi_{yzy} = \chi_{zyy} = \frac{1}{2} N_s \alpha_{ccc} [\cos\theta - \cos^3\theta](1 - r) \tag{5}$$

$$\chi_{zzz} = N_s \alpha_{ccc} [r\cos\theta + \cos^3\theta(1 - r)] \tag{6}$$

The r value for the ester methyl group was determined to be 1.8 in our previous research.[13] Therefore, we have

$$\chi_{xxz} = \chi_{yyz} = N_s \alpha_{ccc} [1.4\cos\theta + 0.4\cos^3\theta] \tag{7}$$

$$\chi_{xzx} = \chi_{zxx} = \chi_{yzy} = \chi_{zyy} = -0.4 N_s \alpha_{ccc} [\cos\theta - \cos^3\theta] \tag{8}$$

$$\chi_{zzz} = N_s \alpha_{ccc} [1.8\cos\theta - 0.8\cos^3\theta] \tag{9}$$

We found from eqs 7−9 that χ_{xzx} and χ_{zxx} are much smaller than χ_{xxz} and χ_{zzz} (see Supporting Information), while χ_{zzz} is in the same order as χ_{xxz}. Since from the previous discussion on ssp SFG spectra, we know that $\chi_{xxz}^{silica/PMA}$ is much smaller than $\chi_{xxz}^{PMA/Ag}$; here we can conclude that $\chi_{xxz}^{silica/PMA}$, $\chi_{xzx}^{silica/PMA}$, $\chi_{zxx}^{silica/PMA}$, and $\chi_{zzz}^{silica/PMA}$ are much smaller than $\chi_{xxz}^{PMA/Ag}$ and thus can be neglected in the data analysis for the ppp spectra. Furthermore, if we inspect the four Fresnel coefficients at the PMA/Ag interface, we find that $|F_{xzx}^{PMA/Ag}|$ (∼0.073) and $|F_{zxx}^{PMA/Ag}|$ (∼0.065) are much smaller than $|F_{xxz}^{PMA/Ag}|$ (∼0.54) and $|F_{zzz}^{PMA/Ag}|$ (∼0.68) (Figure 4). Therefore, the ester methyl symmetric stretching peak at 2955 cm^{-1} in the ppp spectra is dominated by the contributions from $\chi_{xxz}^{PMA/Ag}$ and $\chi_{zzz}^{PMA/Ag}$ at the PMA/Ag interface.

We calculated the Fresnel coefficients of the PMA/fused silica and PMA/Ag interfaces as a function of film thickness in the ppp spectra (Figure 4). The calculated results indicate that Fresnel coefficients for the PMA/Ag interface is independent of the PMA film thickness, while those for the PMA/fused silica interface have substantial changes as a function of film thickness. Figure 2b shows that the experimentally observed SFG ppp spectra do not depend on the film thickness; therefore, they should be contributed solely from the PMA/Ag interface, not the PMA/fused silica interface or both the two interfaces.

Theoretically, we should be able to deduce the tilt angle of the ester methyl groups at the PMA/Ag interface from the measured ratio of $\chi_{ssp}^{PMA/Ag}$ over $\chi_{ppp}^{PMA/Ag}$ since both the ssp and ppp spectra

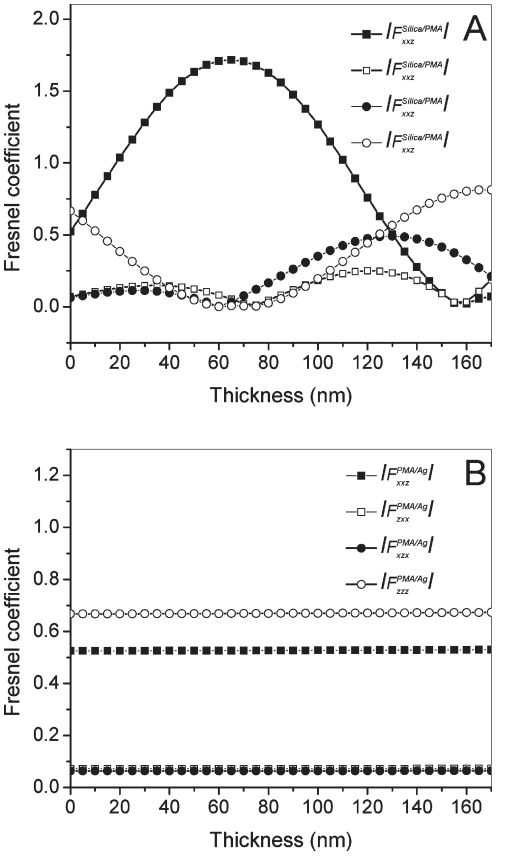

Figure 4. Absolute Fresnel coefficients calculated for the silica/PMA interface (A) and the PMA/Ag interface (B) as a function of the PMA thickness for the ppp spectra.

are dominated by the ester methyl symmetric resonant signals at the PMA/Ag interface. However, when we calculated the Fresnel coefficients of the two interfaces, we need to use the refractive indices of PMA at the PMA/Ag interface. We assumed that they are the same as those of the bulk PMA. In reality, the refractive index of the interfacial layer may be different from that of the bulk material.[48,49] How to evaluate the interfacial refractive index to minimize the error in the data analysis to deduce the functional group orientation has been extensively discussed.[48,49] Here we would not quantify the tilt angle of the ester methyl groups at the PMA/Ag interface. Instead, we want to determine its absolute orientation, that is, whether the ester methyl groups at the PMA/Ag interface tilt toward the PMA bulk or the Ag substrate.

It has been reported previously that in SFG experiments a metal surface can generate large nonresonant background signal which can interfere with the SFG resonant signals.[50] The relative phase between the nonresonant background and the resonant peak can help deduce the absolute orientation direction (away or toward) of the detected functional groups since they can interfere with each other constructively or destructively based on their relative phase.[23,50,51] A self-assembled monolayer of methyl 3-mercaptopropionate (MMP) was prepared on the Ag substrate. A SFG ssp spectrum was collected from such a layer (Figure 5), in which a negative peak at 2955 cm^{-1} was observed. This peak is contributed from the ester methyl symmetric stretching mode. The negative peak indicates that this mode has a different phase compared to the Ag nonresonant background. This is the same as what was observed from the ester methyl group symmetric stretching mode at the PMA/Ag interface, indicating that the ester methyl groups in the two cases adopt the same absolute orientation. As shown in Table 1 and Table 2, the phase differences between the nonresonant

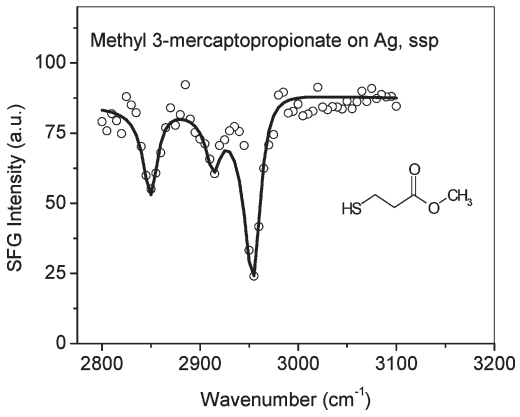

Figure 5. SFG ssp spectrum collected from a self-assembled monolayer of methyl 3-mercaptopropionate on the Ag substrate surface.

Table 2. Fit Parameters for SFG ssp Spectrum Collected from a Self-Assembled Monolayer of MMP on the Ag Substrate Surface (Figure 5)

2955 cm^{-1}		2914 cm^{-1}		2850 cm^{-1}			
A_i	Γ_i	A_i	Γ_i	A_i	Γ_i	χ_{NR}	phase (rad)
46 ± 3	10	10 ± 2	9	17 ± 2	9	9.3 ± 0.2	-1.4 ± 0.1

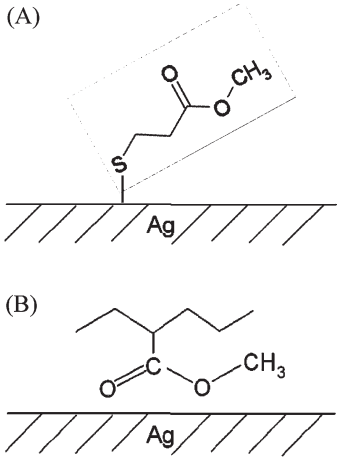

Figure 6. Possible conformations of the ester methyl groups of MMP on Ag surface (A) and of PMA at the PMA/Ag interface.

background and the resonant ester methyl symmetric stretching for both the silica/PMA/Ag and MMP/Ag systems are ~ -1.4. For the MMP layer, the ester methyl group should tilt away from the Ag surface because of the Ag−S chemical bonds at the interface and the hydrophobicity of the methyl groups (Figure 6a). Therefore, at the PMA/Ag interface, ester methyl groups also tilt away from the Ag surface. This result agrees with our previous study of the PMMA/Ag interface.[42] The ester compounds are widely used in formulations of adhesion promoters for adherence to metals. The observed interfacial order and interfacial absolute orientation would favor exposing the electronegative oxygen atoms to the Ag side and help form strong interactions between the metal and the ester groups, as depicted in Figure 6B.

4. Conclusion

In this paper, we demonstrated that polymer molecular order at a buried polymer/metal interface can be directly probed by SFG. Using a PMA film sandwiched between a fused silica surface and a silver surface, we showed that SFG signals collected from the PMA film do not depend on the film thickness. By evaluating the Fresnel coefficients of the fused silica/PMA and PMA/Ag interfaces, we concluded that SFG signals are dominated from the polymer/metal interfaces in both ssp and ppp spectra. The SFG spectra are dominated by the symmetric stretching signal from the ester methyl groups in PMA. According to the SFG phase measurement, absolute orientations of functional groups at interfaces can be deduced. Compared to the SFG signal collected from a MMP monolayer on Ag, it was found that ester methyl groups tilt away from the Ag at the PMA/Ag interface. It is important to investigate molecular structures of interfaces because they determine interfacial properties. We believe that this research will impact studies on polymer/metal interfaces as well as other organic/metal interfaces and organic/metal hybrid materials, which are important in many important application areas of composites, coatings, and modern electronics.

Acknowledgment. This work is supported by NSF (CHE-0449469), SRC (P10419), Dow Corning Corporation, University of Michigan, Nanjing University, and Henkel. Daiwei Li is supported by a CSC fellowship.

Supporting Information Available: More discussions on Fresnel coefficients and second-order nonlinear susceptibility components. This material is available free of charge via the Internet at http://pubs.acs.org.

References and Notes

(1) Feast, W. J.; Munro, H. S.; Richards, R. W. *Polymer Surfaces and Interfaces II*; John Wiley and Sons: New York, 1992.
(2) Carbassi, F.; Morra, M.; Occhiellp, E. *Polymer Surfaces: From Physics to Technology*; John Wiley and Sons: Chichester, 1994.
(3) Jones, R. A. L.; Richards, R. W. *Polymers at Surfaces and Interfaces*; Cambridge University Press: Cambridge, 1999.
(4) Recum, A. F. *Handbook of Biomaterials Evaluation: Scientific, Technical, and Clinical Testing of Implant Materials*; Macmillan: New York, 1986.
(5) Chen, Z.; Shen, Y. R.; Somorjai, G. A. *Annu. Rev. Phys. Chem.* **2002**, *53*, 437–465.
(6) Zhang, D.; Ward, R. S.; Shen, Y. R.; Somorjai, G. A. *J. Phys. Chem. B* **1997**, *101*, 9060–9064.
(7) Opdahl, A.; Somorjai, G. A. *Langmuir* **2002**, *18*, 9409–9412.
(8) Ophahl, A.; Phillips, R. A.; Somorjai, G. A. *Macromolecules* **2002**, *35*, 4387–4396.
(9) Wei, X.; Zhuang, X.; Hong, S.-C.; Goto, T.; Shen, Y. R. *Phys. Rev. Lett.* **1999**, *82*, 4256–4259.
(10) Wei, X.; Hong, S.-C.; Zhuang, X.; Goto, T.; Shen, Y. R. *Phys. Rev. E* **2000**, *62*, 5160–5172.
(11) Kim, D.; Oh-e, M.; Shen, Y. R. *Macromolecules* **2001**, *34*, 9125–9129.
(12) Hong, S.-C.; Zhang, C.; Shen, Y. R. *Appl. Phys. Lett.* **2003**, *82*, 3068–3070.
(13) Wang, J.; Chen, C.; Buck, S. M.; Chen, Z. *J. Phys. Chem. B* **2001**, *105*, 12118–12125.
(14) Wang, J.; Woodcock, S. E.; Buck, S. M.; Chen, C.; Chen, Z. *J. Am. Chem. Soc.* **2001**, *123*, 9470–9471.
(15) Wang, J.; Paszti, Z.; Even, M. A.; Chen, Z. *J. Am. Chem. Soc.* **2002**, *124*, 7016–7023.
(16) Chen, C.; Wang, J.; Even, M. A.; Chen, Z. *Macromolecules* **2002**, *35*, 8093–8097.
(17) Chen, C.; Wang, J.; Chen, Z. *Langmuir* **2004**, *20*, 10186–10193.
(18) Clarke, M. L.; Wang, J.; Chen, Z. *Anal. Chem.* **2003**, *75*, 3275–3280.
(19) Chen, C.; Wang, J.; Loch, C. L.; Ahn, D.; Chen, Z. *J. Am. Chem. Soc.* **2004**, *126*, 1174–1179.
(20) Loch, C. L.; Ahn, D.; Vazquez, A. V.; Chen, Z. *J. Colloid Interface Sci.* **2007**, *308*, 170–175.
(21) Chen, C.; Loch, C. L.; Wang, J.; Chen, Z. *J. Phys. Chem. B* **2003**, *107*, 10440–1045.
(22) Loch, C. L.; Ahn, D.; Chen, Z. *J. Phys. Chem. B* **2006**, *110*, 914–918.

(23) Loch, C. L.; Ahn, D.; Chen, C.; Wang, J.; Chen, Z. *Langmuir* **2004**, *20*, 5467–5473.
(24) Johnson, W. C.; Wang, J.; Chen, Z. *J. Phys. Chem. B* **2005**, *109*, 6280–6286.
(25) Even, M. A.; Chen, C.; Wang, J.; Chen, Z. *Macromolecules* **2006**, *39*, 9396–9401.
(26) Rao, A.; Rangwalla, H.; Varshney, V.; Dhinojwala, A. *Langmuir* **2004**, *20*, 7183–7188.
(27) Rangwalla, H.; Dhinojwala, A. *J. Adhes.* **2004**, *80*, 37–59.
(28) Zhang, D.; Dougal, S. M.; Yeganeh, M. S. *Langmuir* **2000**, *16*, 4528–4532.
(29) Briggman, K. A.; Stephenson, J. C.; Wallace, W. E.; Richter, L. J. *J. Phys. Chem. B* **2001**, *105*, 2785–2791.
(30) Wilson, P. T.; Briggman, K. A.; Wallace, W. E.; Stephenson, J. C.; Richter, L. J. *Appl. Phys. Lett.* **2002**, *80*, 3084–3086.
(31) Wilson, P. T.; Richter, L. J.; Wallace, W. E.; Briggman, K. A.; Stephenson, J. C. *Chem. Phys. Lett.* **2002**, *363*, 161–168.
(32) Morita, S.; Ye, S.; Li, G.; Osawa, M. *Vib. Spectrosc.* **2004**, *35*, 15–19.
(33) Ye, S.; Morita, S.; Li, G.; Noda, H.; Tanaka, M.; Uosaki, K.; Osawa, M. *Macromolecules* **2003**, *36*, 5694–5703.
(34) Ye, H. K.; Gu, Z. Y.; Gracias, D. H. *Langmuir* **2006**, *22*, 1863–1868.
(35) Jayathilake, H. D.; Zhu, M. H.; Rosenblatt, C.; Bordenyuk, A. N.; Weeraman, C.; Benderskii, A. V. *J. Chem. Phys.* **2006**, *125*, 064706.
(36) Li, Q. F.; Hua, R.; Cheah, I. J.; Chou, K. C. *J. Phys. Chem. B* **2008**, *112*, 694–697.
(37) Li, Q.; Hua, R.; Chou, K. C. *J. Phys. Chem. B* **2008**, *112*, 2315–2318.
(38) Liu, Y.; Messmer, M. C. *J. Phys. Chem. B* **2003**, *107*, 9774–9779.
(39) Miyamae, T.; Nozoye, H. *Surf. Sci.* **2003**, *532*, 1045–1050.
(40) Ye, H.; Abu-Akeel, A.; Huang, J.; Katz, H. E.; Gracias, D. H. *J. Am. Chem. Soc.* **2006**, *128*, 6528–6529.
(41) Ye, H.; Huang, J.; Park, J.-R.; Katz, H. E.; Gracias, D. H. *J. Phys. Chem. C* **2007**, *111*, 13250–13255.
(42) Lu, X.; Shephard, N.; Han, J.; Xue, G.; Chen, Z. *Macromolecules* **2008**, *41*, 8770–8777.
(43) Guyot-Sionnest, P.; Hunt, J. H.; Shen, Y. R. *Phys. Rev. Lett.* **1987**, *59*, 1597–1600.
(44) Wilk, D.; Johannsmann, D.; Stanners, C.; Shen, Y. R. *Phys. Rev. B* **1995**, *51*, 10057–10067.
(45) Feller, M. B.; Chen, W.; Shen, Y. R. *Phys. Rev. A* **1991**, *43*, 6778–6792.
(46) Zhuang, X.; Miranda, P. B.; Kim, D.; Shen, Y. R. *Phys. Rev. B* **1999**, *59*, 12632–12640.
(47) Hirose, C.; Akamatsu, N.; Domen, K. *Appl. Spectrosc.* **1992**, *46*, 1051–1072.
(48) Ye, P.; Shen, Y. R. *Phys. Rev. B* **1983**, *28*, 4288–4294.
(49) Simpson, G. J.; Dailey, C. A.; Plocinik, R. M.; Moad, A. J.; Polizzi, M. A.; Everly, R. M. *Anal. Chem.* **2005**, *77*, 215–224.
(50) Ward, R. N.; Davies, P. B.; Bain, C. D. *J. Phys. Chem.* **1993**, *97*, 7141–7143.
(51) Vázquez, A. V.; Shephard, N. E.; Steinecker, C. L.; Ahn, D.; Spanninga, S.; Chen, Z. *J. Colloid Interface Sci.* **2009**, *331*, 408–416.